

# A Behavioral SPICE Compatible Model of an Electrodeless Fluorescent Lamp

Sam Ben-Yaakov<sup>\*1</sup>, Moshe Shvartsas<sup>1</sup> and Jim Lester<sup>2</sup>

<sup>1</sup>Power Electronics Laboratory  
Department of Electrical and Computer Engineering  
Ben-Gurion University of the Negev  
P. O. Box 653  
Beer-Sheva 84105, ISRAEL  
Phone: +972-8-646-1561; Fax: +972-8-647-2949;  
Email: [sby@ee.bgu.ac.il](mailto:sby@ee.bgu.ac.il)  
Website: [www.ee.bgu.ac.il/~pel](http://www.ee.bgu.ac.il/~pel)

<sup>2</sup>Central Research & Services Laboratories  
Fluorescent Systems Laboratory  
OSRAM SYLVANIA  
71 Cherry Hill Dr.  
Beverly, MA 01915 USA  
Phone: 1-978-750-1605  
FAX: 1-978-750-1790  
EMAIL: [jim.lester@sylvania.com](mailto:jim.lester@sylvania.com)

**Abstract-** A behavioral, SPICE compatible, model was developed for an electrodeless fluorescent lamp (OSRAM SYLVANIA ICETRON/ENDURA 150W). The model emulates the static and dynamic behavior of the lamp when driven at high frequency. The model was tested under various experimental conditions: at steady state for different power levels, with an AM modulated drive, and under transient changes. Good agreement was found between the simulation runs and experimental results. However, the effect of temperature on the lamp's behavior may require a tighter fit of the model to the temperature dependence in cases where large changes in operating condition need to be simulated.

## I. INTRODUCTION

Fluorescent lamps are simply constructed light sources consisting of a glass vessel coated inside with light emitting phosphor. Inside the vessel is a combination of inert gas and Mercury gas. During operation, the Mercury is energized and produces UV, which activates the phosphor and produces light. In an electroded lamp, the Mercury is energized by the current delivered through the electrodes [1]. In an electrodeless lamp, power must be delivered to the lamp either inductively or capacitively. Most commercial electrodeless lighting products today use inductive coupling and low operating frequencies where power conversion is most efficient.

There are many shapes used in electrodeless lamps [2, 3]. Each shape offers a different optical or efficiency advantage. Some lamps are spherical in shape with the inductive coupling coil inside the lamp protected by a glass re-entrant cavity. Some spherical lamps have the coil surrounding the lamp. This paper will examine the oval or racetrack shaped lamp shown in Fig. 1, which uses two inductive coupling coils connected in parallel. The physics of this lamp has been discussed in recent papers [4 - 7]. This paper will examine a

PSPICE circuit model for the lamp construction of Fig. 1, which can be used in circuit simulations. The results can be applied to other electrodeless lamp shapes.

The objective of this study was to develop a SPICE compatible model that will exhibit two major electrical features of an electrodeless fluorescent lamp operated at HF: the dependence of the lamp's resistance on power level and its dynamic response to changes in electrical excitation. Based on an earlier methodology, which relies on experimental observations as well as some physics based reasoning, a behavioral model was developed to emulate the electrical response of the electrodeless fluorescent lamp. Once developed, the model was calibrated against experimental data and then verified by independent measurements.

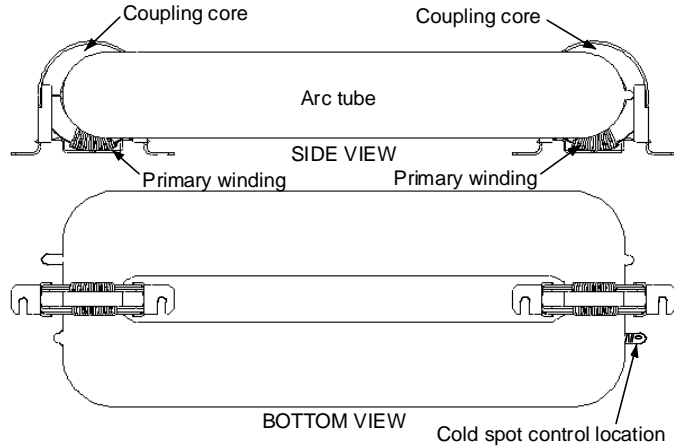
## II. THE BEHAVIORAL MODEL OF ELECTRODELESS FLUORESCENT LAMP

The proposed model is based on the assumption that the fundamental behavior of an electrodeless fluorescent lamp is similar to the behavior of a lamp with hot electrodes. The only difference being the way the electrical energy is coupled to the plasma. In the case of the lamp with electrodes, coupling is via wires. In the case of the electrodeless lamp of the ICETRON/ENDURA type, coupling is by magnetic induction. It was thus assumed that the model concept developed earlier [8] will fit the case of the electrodeless lamp.

As reported in an earlier study [9], the impedance of a fluorescent lamp operated at high frequency is, to a first order approximation, resistive. That is, at any given operation point, the current of the lamp's arc tube can be expressed as:

$$I_{\text{lamp}} = \frac{V_{\text{lamp}}}{R_{\text{eq}}} \quad (1)$$

\* Corresponding author



1. Physical ICETRON/ENDURA construction.

where:

$I_{lamp}$  – lamp current

$V_{lamp}$  – lamp voltage

$R_{eq}$  – equivalent resistance of the lamp when driven at high frequency

However, the equivalent resistance  $R_{eq}$  is a function of the operating point, namely, of the rms current of the lamp. This dependence can be easily obtained for a given lamp by measuring rms voltages and rms currents of the lamp over the modeled operating range [5, 10]. Based on these simple observations, the behavioral model can be developed by applying behavioral dependent voltage (or current) sources available in any modern electronic circuit simulators. The model (Fig. 2) describes the lamp as a dependent current source (G1) that emulates a variable resistance according to (1). The expression of the G1 function is the voltage across the lamp at any given point, divided by  $R_{eq}$  which is expressed as a function of the rms current of the lamp:

$$G_1 = \frac{V_{lamp}}{R_{eq}(i(rms))} \quad (2)$$

The output of the dependent voltage source E1 is proportional to the square of the lamp current ( $i(lamp)$ ).

$$E_1 = \{i(lamp)\}^2 \quad (3)$$

The resulting voltage signal  $\{v(isq)\}$  at node (isq) is then passed through a low pass filter ( $R_1C_1$ , Fig. 2) to obtain its low frequency component. For frequencies  $f > 1/(2\pi R_1C_1)$  and for times  $t > R_1C_1$  the average voltage on  $C_1$  (node (p)) will be:

$$v(p) = \frac{1}{T} \int_0^T v(isq) dt = \frac{1}{T} \int_0^T [i(lamp)]^2 dt \quad (4)$$

where T is the time constant  $R_1C_1$ .

The filtered  $I_{rms}$  is then obtained by E2 (node 'rms' in Fig. 2) as the square root of the average voltage across the capacitor C1 (node 'p'): The filtered  $I_{rms}$  is then obtained by E2 (node 'rms' in Fig. 2) as the square root of the average voltage across the capacitor C1 (node 'p'):

$$E_2 = \sqrt{v(p)} \quad (5)$$

Consequently, the voltage at node rms,  $v(rms)$  is equal to the numerical value of the rms current of the lamp. This voltage, is then used in the expression of  $R_{eq}(v(rms))$  to calculate the lamp's current by (1). The function  $R_{eq}(v(rms))$  is based on a numerical fitting of  $R_{eq}$  as a function of the lamp current. Various fitting templates have been used in the past [8,10,11]; linear fitting as well as high order polynomial fitting. In this study we explored an exponential fitting that was found to yield a good match to the experimental data (Fig. 3).

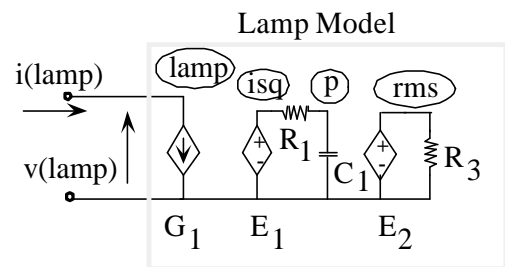
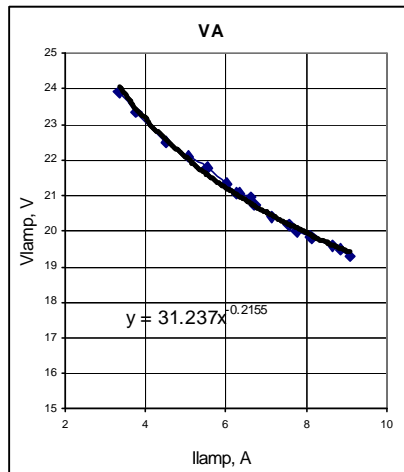
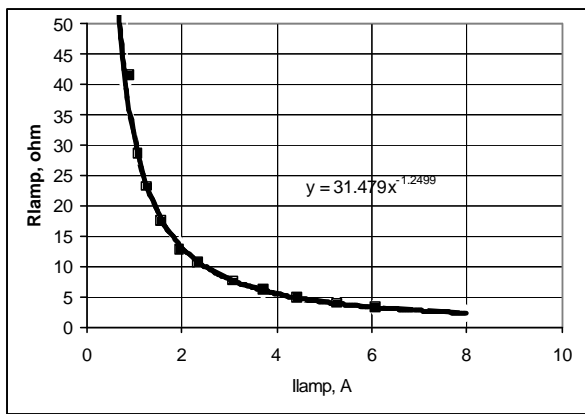


Fig. 2. Proposed fluorescent lamp model.



(a)



(b)

Fig. 3. Experimental curve fitting of the ICETRON/ENDURA 150W. (a) V-A curve. (b) Req.

### III. EXPERIMENTAL SET UP

The experimental set up (Fig. 4a) was built around a parallel resonant inverter similar to the electrodeless lamp ballast described in [6]. It included a half bridge inverter (M1, M2), resonant network ( $L_r$ ,  $C_r$ ) and a 50  $\Omega$  resistor in parallel to a bi-directional switch (M3, M4). The switch was used to inject a disturbance in the lamp's current. That is, by shorting and releasing the 50  $\Omega$  resistor, the lamp current was slightly modulated and the dynamic response could be watched. An RC snubber ( $R_{sn}$ ,  $C_{sn}$ ) was placed around the switch to absorb the spikes due to the hard switching. The lamp voltage was measured by extra windings on the toroid transformers used to drive the electrodeless lamp (Lt1 and Lt2 of Fig. 4a) [4, 5]. The current of the lamp was measured by a current transformer that was built in house (Fig. 4a), shunted by a 100  $\Omega$  resistor ( $R_{sh}$ ).

The simulation model (Fig. 4b) was made to follow as close as possible the experimental set up. However, in the

interest of saving simulation run time, the inverter was replaced by a square-wave voltage source (V1+LIMIT) while the modulating bi-directional switch was replaced by an "ideal" switch (S1). The simulation model included 2 transformers (coupled inductors) to drive the lamp, emulating the toroid drivers. The lamp was represented by a dependent current source (G1, connected between the nodes el1, el2) and the additional behavioral sources (E1 – E3) per the model of Fig. 2.

### IV. MODEL CALIBRATION

The parameters of the model for the ICETRON/ENDURA 150W lamp were calibrated experimentally. The equivalent resistance of the lamp  $R_{eq}$  was obtained by measuring voltages and currents of the lamp over a current range of 0.8A to 9 A. Typical results are shown in Figs. 3a,b. Several approaches were used to fit the functional relationship between  $R_{eq}$  and the lamp's rms current. They include linear and polynomial fitting [8,10,11], table fitting (applying the ETABLE behavioral source of ORCAD), and an exponential curve fit. Best matching, over a large lamp current range, was obtained with an exponential fitting.

The numerical expression for the equivalent resistance of the ICETRON/ENDURA 150W lamp was found to be:

$$R_{eq} = 31.479 (I_{lamp})^{1.2499} \quad (6)$$

The time constant  $R_1C_1$  of the model (Fig. 2) was calibrated by exposing the lamp to a current transient. This was done by the experimental circuit of Fig. 4a against the simulation model of Fig. 4b. The time constant was found to be 75  $\mu$ s.

### V. EXPERIMENTAL RESULTS

The degree of matching between the static experimental results and model simulation are shown in Fig. 5 for the time domain signal, and in Fig. 6 for the static V-A curve. The dynamic response was observed by driving the modulating switch (M3, M4 of Fig. 4a, S1 of Fig 4b) at various frequencies. A typical response of the lamp to the modulation is shown in Fig. 7. Figure 7b is a zoomed picture of the voltage and current disturbances.

Notice that when modulated, the incremental impedance  $V_{lamp}/I_{lamp}$  is negative ( $V$  and  $I$  in opposite phases). The magnitude of this incremental impedance was used to calibrate the dynamic parameters of the model, that is the  $R_{int}C_{int}$  time constant (Fig. 4b).  $R_{int}$  was kept at 1k  $\Omega$  while  $C_{int}$  was iterated to find the best fit against the experimental data. It was found that a capacitance range of 75nF to 150nF yielded a good match. This corresponds to a time constant range of 75  $\mu$ s to 150  $\mu$ s, corresponding to a bandwidth range of approximately 1kHz to 2kHz. The degree of matching between the simulation and experimental results is shown in Figs. 8-10 for the modulating frequency range of 300Hz to 20kHz.

The modulation experiments as well as the simulation clearly show the (modulating) frequency dependence of the incremental impedance [8, 10, 11]. At 2kHz (Fig. 9), the incremental impedance is already slightly positive and becomes larger as the modulating frequency increases. The dependence of the incremental impedance on the modulating frequency, measured in this study, is summarized in Fig. 11. It is apparent from this summary that the 150nF value for  $C_{int}$  is somewhat a better choice (corresponding to a time constant of about to 150 s).

Notwithstanding the excellent match between the experimental data and the simulation results, it was observed that the lamp's parameters are temperature dependent. A cursory examination of this issue was carried out by repeating the V-A curve measurements while a fan cooled the lamp. The results (Fig. 12) show a rather large dependence on the surface temperature of the glass tube as perhaps would be expected considering the large surface area of the lamp.

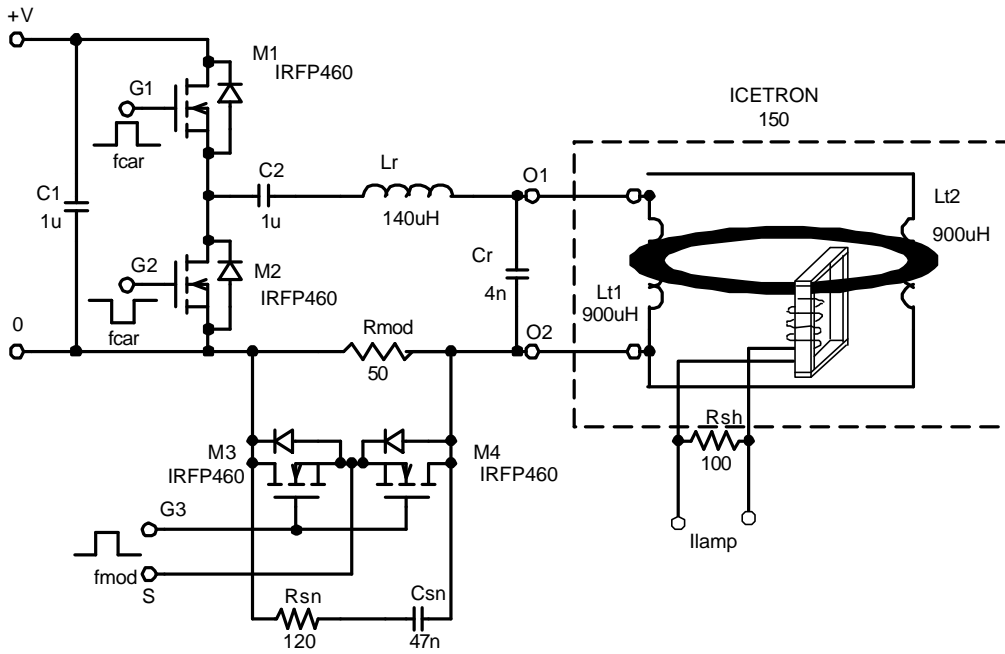
## VI. DISCUSSION AND CONCLUSIONS

The behavioral model developed through this study was found to faithfully emulate the static and dynamic behavior of the ICETRON/ENDURA electrodeless fluorescent lamp. The model emulates well the static behavior of the lamp both at nominal operating condition and under dimmed conditions. The model also emulates well the negative incremental lamp impedance at a low modulating frequency and the positive impedance at a high modulating frequency. The preliminary investigation of the temperature dependence of the lamp's parameters shows that the lamp is rather sensitive to temperature. Consequently, the simulation model presented here is valid for the temperature condition that prevailed while the model was calibrated. By repeating the calibration over a number of temperature points, and making the parameters of the model temperature dependent, it would be possible to generate a universal model that is valid over a given temperature range.

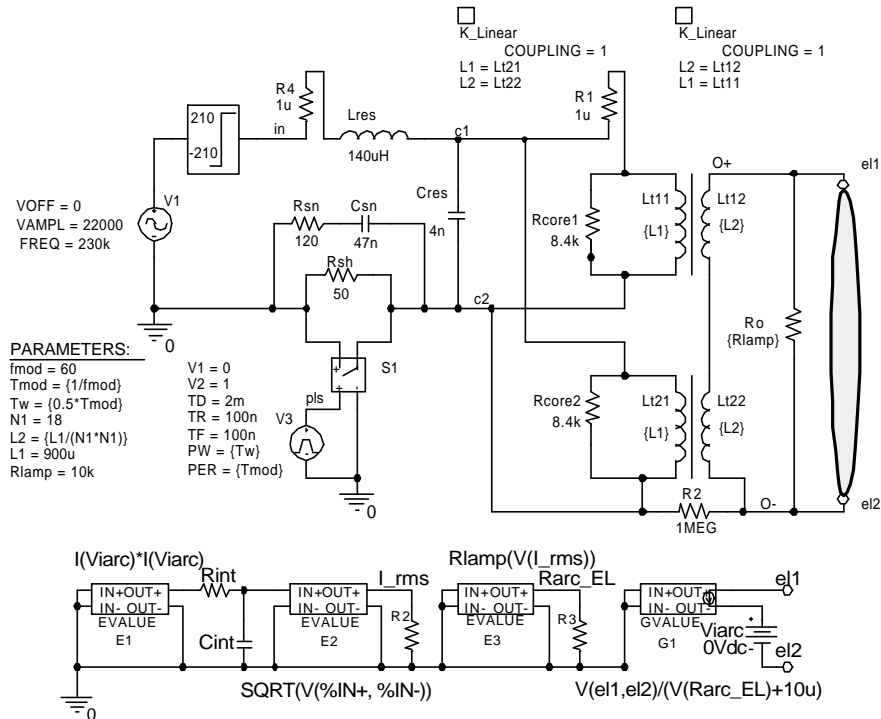
It is suggested that the proposed model could be useful in the design phase of electronic ballasts for the electrodeless fluorescent lamp and in particular in the design of dimming and closed loop control for such systems. The model does not cover the process of ignition and some further calibration and fitting will be required to match the behavioral model to the physical lamp for wide temperature range applications.

## REFERENCES

- [1] W. Elenbaas, Ed., *Fluorescent Lamps*, Macmillan, London, 1971.
- [2] Lighting Research Center, "Electrodeless Lamps, The Next Generation," *Lighting Futures*, vol. 1, no. 1, May/June 1995.
- [3] Wharmby, D. O., "Electrodeless lamps for lighting: a review", *IEE PROCEEDINGS-A*, 140 (No. 6), pp.465-473, 1993.
- [4] J. W. Shaffer and V. A. Godyak, "The Development of Low Frequency, High Output Electrodeless Fluorescent Lamps," *Journal of the IES*, vol. 28, no. 1, p142, Winter 1999.
- [5] R.B. Piejak, V. A. Godyak, and B.M. Alexandrovich, "A Simple Analysis of an Inductive RF Discharge," *Plasma Sources Sci. Technol.* 1, pp. 179 -186, 1992.
- [6] J. N. Lester and B. A. Alexandrovich, "Ballasting Electrodeless Fluorescent Lamps", *Journal of the IES*, vol. 29, no. 2, pp 89-99, Summer 2000.
- [7] OSRAM SYLVANIA INC., "ICETRON, Fixture Design Guide 100 Endicott St.," Danvers, MA, 01923.
- [8] S. Ben-Yaakov, M. Shvartsas, and S. Glozman, "Static and dynamic of fluorescent lamps operating at high frequency: Modeling and simulation," *IEEE Applied Power Electronics Conference, APEC-99*, pp. 467-472, Dallas, 1999.
- [9] E. E. Hammer, "High frequency characteristics of fluorescent lamp up to 500kHz," *Journal of the Illuminating Engineering Society*, pp. 52-61, Winter, 1987.
- [10] M. Gulko and S. Ben-Yaakov, "Current-sourcing parallel-resonance inverter (CS-PPRI): Theory and application as a fluorescent lamp driver," *IEEE Applied Power Electronics Conference, APEC-93*, pp. 411-417, San-Diego, 1993.
- [11] S. Glozman and S. Ben-Yaakov, "Dynamic interaction of high frequency electronic ballasts and fluorescent lamps. *IEEE Transactions on Industry Applications*, Vol. 37. 2001 pp. 1531-1536, 2001.



(a)



(b)

Fig. 4. Experimental set-up used to extract the dynamic parameter  $R_1C_1$  of the lamp model (a), and the corresponding lamp simulation model (b).

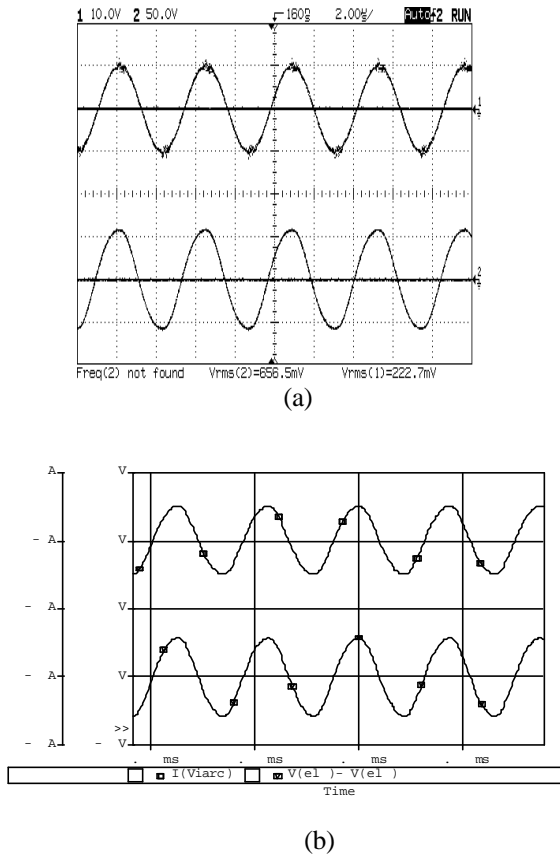


Fig. 5. Lamp current (upper traces and voltage (lower traces) for the ICETRON/ENDURA 150W; Drive frequency: 228kHz. (a) Experiment – 7.119A/20.9V; (b) SPICE simulation – 7.12A/20.47V

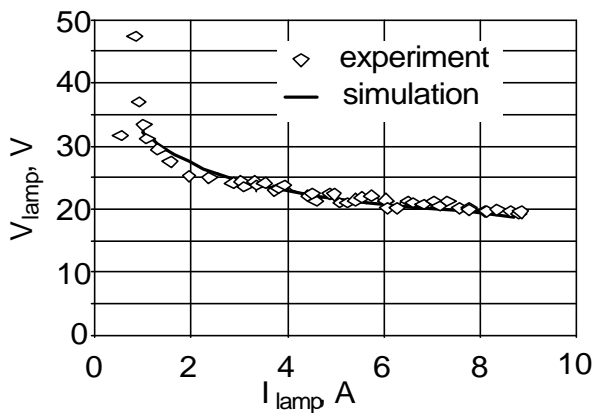


Fig. 6. V-A curves of the ICETRON/ENDURA 150W lamp. Model simulation and experiment.

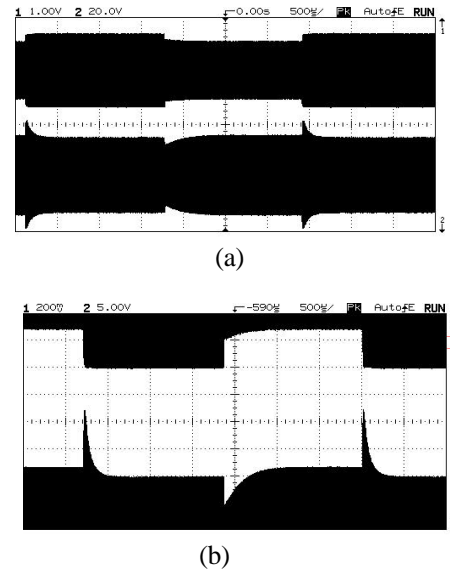


Fig. 7. Dynamic response of ICETRON 150W to a modulated current. Modulation frequency = 340Hz; Upper traces: voltage, lower traces: current. (a) Measured. (b) Measured – Zoomed

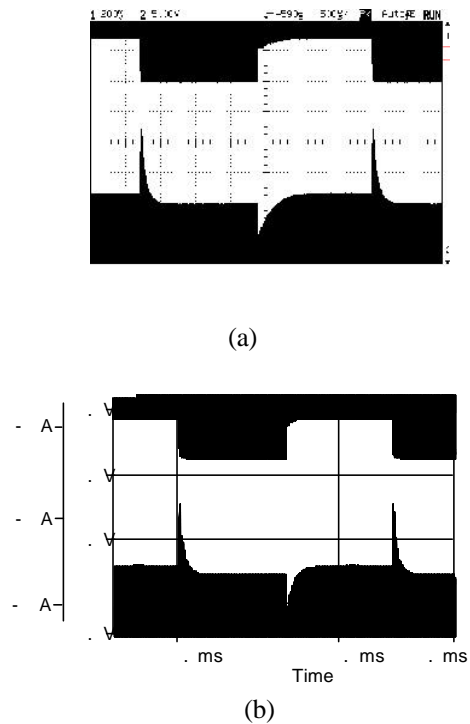


Fig. 8. Dynamic response of ICETRON 150 to modulated current.  $f_{mod}=300$  Hz; Upper trace – current; lower – voltage. (a) – experiment; (b) – simulation,  $C_{int}=75nF$

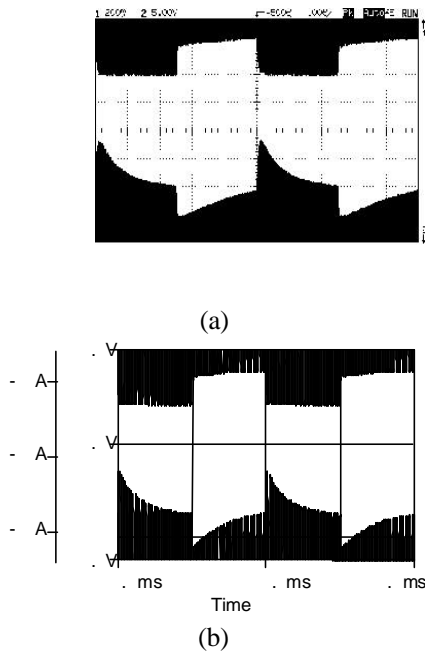


Fig.9. Dynamic response of ICETRON 150 to modulated current.  $f_{mod}=2\text{kHz}$   
Upper trace – current; lower – voltage. (a) – experiment; (b) – simulation,  $C_{int}=75\text{nF}$

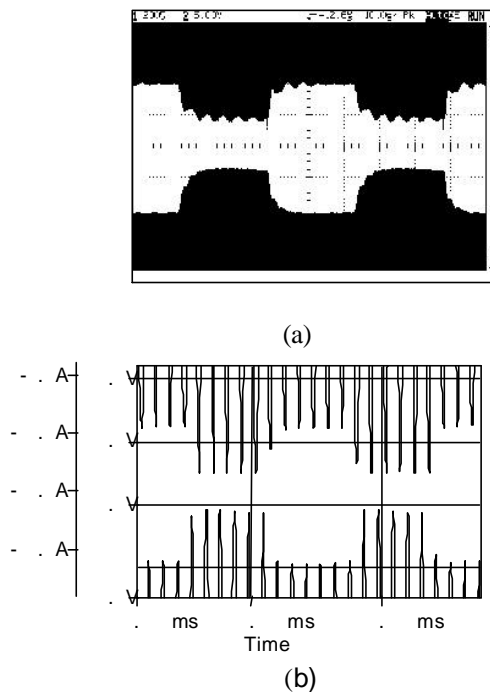


Fig.10. Dynamic response of ICETRON 150 to modulated current.  $f_{mod}=20\text{Hz}$   
Upper trace – current; lower – voltage. (a) – experiment; (b) – simulation,  $C_{int}=75\text{nF}$ .

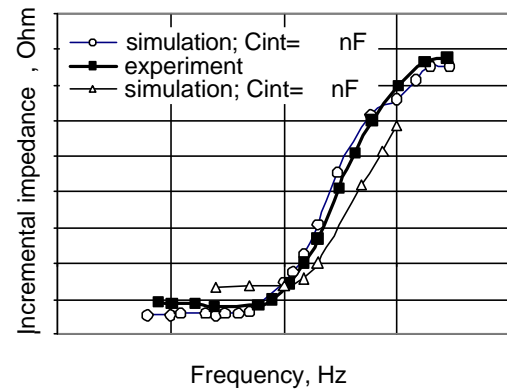


Fig. 11. Incremental impedance. Experiment and simulation results.

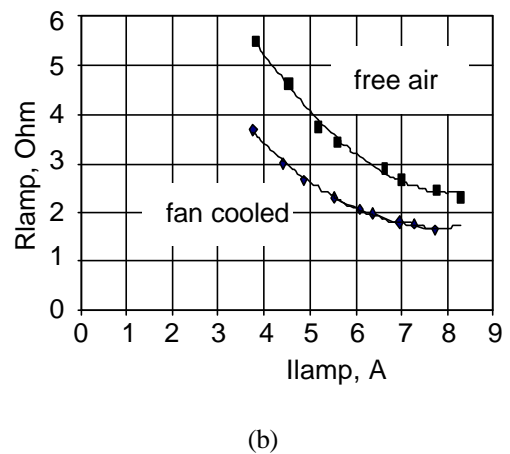
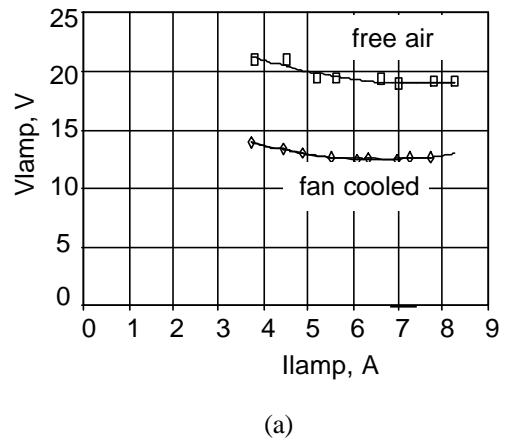


Fig.12. Lamp dependence on cooling conditions. (a) V-A curve. (b) Equivalent resistance.